Numerical Investigation of Angulation Effects in Stenosed Renal Arteries

Mortazavinia Z.[1], Arabi S.[1], Mehdizadeh A. R.[*2]

[1]Department of Mechanical Engineering, ÉcolePolytechnique de Montréal, Montréal, Canada
[2]Center for Research in Medical Physics and Engineering, School of Medicine, Shiraz University of Medical Science, Shiraz, Iran

ABSTRACT

Background: Numerical study of angulation effects of renal arteries on blood flow has been of great interest for many researchers.

Objective: This paper aims at numerically determining the angulation effects of stenosed renal arteries on blood flow velocity and renal mass flow.

Method: An anatomically realistic model of abdominal aorta and renal arteries is reconstructed from CT-scan images and used to conduct numerical simulation of pulsatile non-Newtonian blood flow incorporating fluid-structure interaction. The renal arteries in the realistic model have left and right branch angles of 53˚ and 45˚, respectively. Atrapezium shape stenosis is considered in the entrance of right renal artery. Two other branch angles, i.e. 90˚ and 135˚, are also considered for right renal artery to study the angulation effects.

Results: Comparison between models with right renal branch angles of 45˚, 90˚ and 135˚ reveals that high curvature of streamlines in the entrance of the renal artery with the angle of 135˚ causes the flow velocity and renal mass flow to be less than those of 45˚and 90˚.

Conclusion: It is concluded that large renal branch angles cause the arteries to be unable to deliver blood in the requisite amounts to kidney. Kidney responds to counteract low blood flow by activating the renin-angiotension system which leads to severe hypertension.

Keywords

Angulation, Renal arteries,Renal mass flow, Hypertension, Fluid-structure interaction

Introduction

Detailed knowledge of blood flow and response of blood vessels is necessary to prevent, diagnose, and treat cardiovascular diseases which are the main causes of death in developed countries[1]. Hypertension or high blood pressure is a cardiac condition in which the systemic blood pressure is elevated. Hypertension is classified as essential or secondary hypertension [2]. No medical cause has been found for essential hypertension [3]. Secondary hypertension results from identifiable causes such as endocrine diseases, kidney diseases, coarctation of the aorta and tumors [2].

One to five percent of hypertensive patients are affected by renal artery stenosis (RAS) which is the most common secondary cause of hypertension [4]. RAS is of great clinical interest and extensive experimental and computational studies have been performed to determine the effects of RAS on blood flow characteristics. Liang *et al*. [5] studied the fluid

*Corresponding author: Mehdizadeh A. Assistant Professor of Medical Physics
Room No. 702, Department of Medical Physics, School of Medicine, Shiraz University of Medical Science, Shiraz, Iran.
E-mail: mehdizade@sums.ac.ir

dynamics in normal and stenosed human renal arteries to assess hemodynamic factors associated with RAS. Kagadis *et al*. [6] simulated Newtonian blood flow across rigid RAS and investigated the effects of RAS on velocity, flow rate, overall pressure drop and wall shear stress. Schoenberg *et al*. [7] and Westenberg *et al*. [8] observed that changes in hemodynamic significance of the stenosis affect the blood flow waveform in the stenosed renal artery.

Besides the existence of stenosis in renal arteries which can impede blood flow to the kidney [9], geometric properties such as renal branch angles are also critical parameters which affect blood flow characteristics through renal arteries [10]. Renal branch angle may be one of the factors that causes the arteries to be not able to deliver blood in the requisite amounts to the kidney and leads to decreased renal mass and perfusion pressure. Response of the kidney to counteract low blood flow is activation of renin-angiotension system which leads to severe hypertension [9,11]. Thus, it is an important issue for furthur investigation. Unfortunately, limited numerical studies have been carried out on the effects of renal branch angle on blood flow through renal arteries.

This paper aims at numerically determining the angulation effects of stenosed renal arteries on blood flow velocity and renal mass flow rate. In order to achieve this, an anatomically realistic model of abdominal aorta and renal arteries is reconstructed from CT scans, and used to conduct computational simulation of pulsatile non-Newtonian blood flow incorporating fluid-structure interaction (FSI). The angle between the aorta and the right renal artery in the realistic model is 45°. Two other branch angles, i.e. 90° and 135° are also considered for right renal artery to study the effects of angulation. Incorporating FSI in studying stenosed arteries provides a valuable tool in determining critical areas where plaque rupture or vessel wall collapse is likely to occur. In the present study, an iterative two-way coupling method is employed to link the fluid and solid portions. To achieve this, ANSYS 13.0 software package containing the finite element and finite volume-based commercial codes, ANSYS Workbench and CFX, is used to simulate the structural and fluid domains, respectively.

Materials and Methods

Governing equations

The blood flow in the vessels is usually laminar. This is the normal condition for blood flow throughout most parts of the circulatory system. Turbulent flow, however, occurs at highly stenosed vessels, highly irregular flow paths and under conditions of high flow, particularly in the ascending aorta [12].

For unsteady laminar flow of an incompressible fluid, the mass and momentum equations (ignoring body forces) can be written as [13]:

$$\frac{\partial U_i}{\partial x_i} = 0 \qquad (1)$$

$$\frac{\partial U_i}{\partial t} + \frac{\partial (U_i U_j)}{\partial x_j} = \frac{1}{\rho_f}\left[-\frac{\partial p}{\partial x_i} + \frac{\partial}{\partial x_j}\left(\mu \left(\frac{\partial U_i}{\partial x_j} + \frac{\partial U_j}{\partial x_i} \right)\right)\right] \qquad (2)$$

where U_i denotes velocity components, ρ and μ are fluid density and viscosity, respectively and p is the pressure.

For the vessel wall, which is defined as an elastic solid, the stress and displacement relationship (ignoring body forces) can be mathematically expressed as [13]:

$$\rho_w \frac{\partial^2 d_i}{\partial t^2} = \frac{\partial \sigma_{ij}}{\partial x_j} \qquad (3)$$

where d_i and σ_{ij} are the components of the displacements and stress tensor in solid, respectively, and ρ_w is the wall density. Similarly, σ_{ij} can be obtained from the constitutive equation of the material. For a Hookean elastic solid, it is as follows [13]:

$$\sigma_{ij} = \lambda e_{kk}\delta_{ij} + 2\mu_L e_{ij} \qquad (4)$$

where λ and μ_L are the Lame's constants, δ_{ij} is the Kronecker delta and e_{ij} are the components of the strain tensor which can be expressed as [13]:

$$e_{ij} = \frac{1}{2}\left(\frac{\partial d_i}{\partial x_j} + \frac{\partial d_j}{\partial x_i}\right) \quad (5)$$

Lame's constants are related to physical material properties, Young's modulus, E, and Poisson's ratio, υ, by the following equations[13]:

$$\lambda = \frac{\upsilon E}{(1+\upsilon)(1-2\upsilon)} \quad (6)$$

$$\mu_L = \frac{E}{2(1+\upsilon)} \quad (7)$$

Geometry

An anatomically realistic model of healthy abdominal aorta and renal arteries, which is from CT-scan images, is shown in figure 1. Figure 2 shows the basic model geometry used in this study which is reconstructed from figure 1, using a computer-aided design (CAD) software. The inlet and outlet diameters of main aorta are 18 and 13 mm, respectively. Also, outlet diameters of left and right renal arteries are 5 and 4 mm, respectively. The wall thicknesses of aorta and renal arteries are not equal and they are set to have the values of 2 and 1 mm, respectively [12].

It has been shown that in the renal artery of humans, RAS commonly occurs in the upstream portion 1 to 2 cm distal to the renal ostium [10]. In this study, an axisymmetric trapezium shape stenosis with a length of L=1 cm and area reduction of 45% is considered in the entrance of right renal artery, as depicted in figure 3.

The renal arteries in the realistic model have

Figure 1: CT-scan images of Abdominal aorta and renal arteries

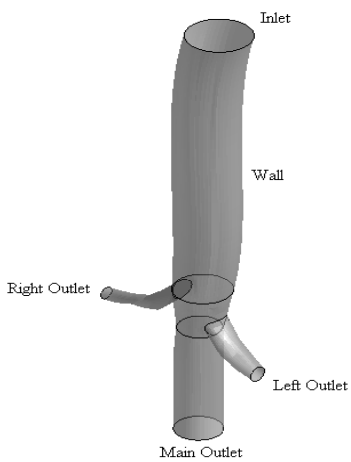

Figure 2: Basic model geometry, reconstructed from CT-scan images

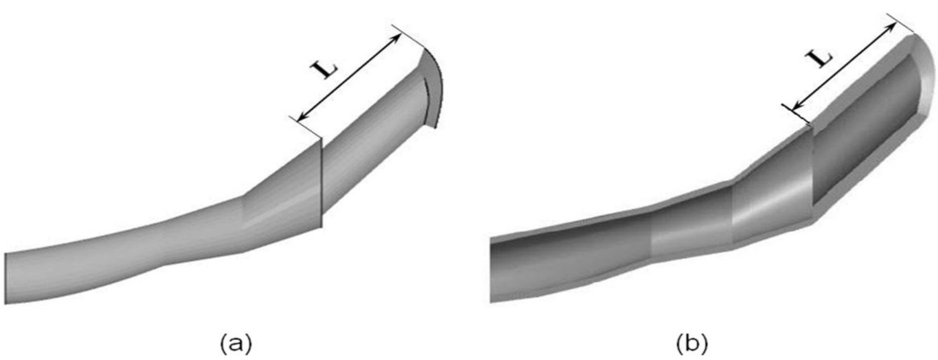

Figure 3: Stenosed right renal artery (a) flow field (b) vessel wall

left and right branch angles of 53° and 45°, respectively. In addition, two other branch angles, i.e. 90° and 135°, are also considered for right renal artery to investigate the effects of angulation as shown in figure 4.

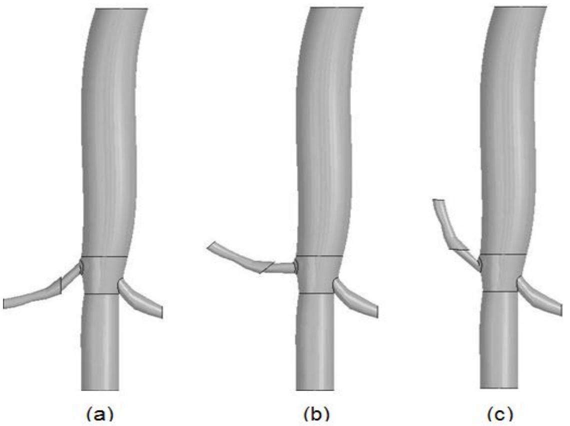

Figure 4: Basic model geometry with different right renal branch angles of (a)45° (b)90° (c) 135°

It is necessary to have proper mesh to reflect actual conditions and provide accurate answers while not exceeding reasonable computational power. Due to the geometry complexity, multi-block meshing technique is used to create structured mesh in computational domains and to prevent high grid concentration in the centre of circular cross sections (as shown in figure 5). The generated structured grid consists of 498,790 hexahedral elements, by performing grid study.

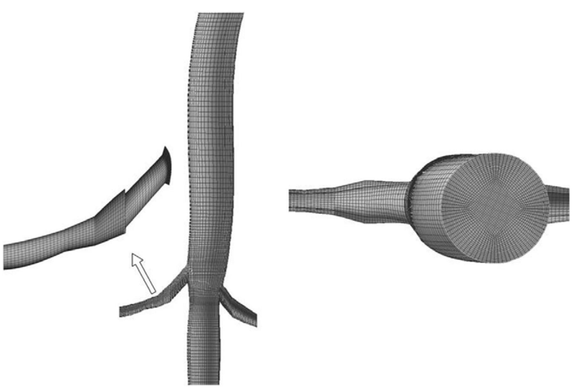

Figure 5: Structured mesh for computational domain

Material Properties

Several models have been proposed to predict the stress–strain relationship for blood [14-17]. However, none of these models is generally accepted as a reflection of the true behavior of the rheology of blood. The Carreau non-Newtonian model, as used by Cho and Kensey [15] and Johnston *et al*. [16] has been seen to provide close approximations to experimental blood flow conditions and not over-predict the non-Newtonian effects. Therefore, this model is used in the present study. The relation between viscosity and shear strain rate, $\dot{\gamma}$, can be written as [16]:

$$\mu = \mu_\infty + (\mu_0 - \mu_\infty)\left[1 + (\lambda_f \dot{\gamma})^2 \right]^{(n-1)/2} \quad (8)$$

where $\lambda_f = 3.313\,\mathrm{s}$, zero strain viscosity $\mu_0 = 0.056\ \mathrm{Pa.s}$, infinite strain viscosity $\mu_\infty = 0.00345\ \mathrm{Pa.s}$, and the empirical exponent $n = 0.3568$.

Also the blood has a density of 1050 kg/m^3 and the vessel is considered to be linearly elastic, isotropic and nearly incompressible with a Young's modulus of 4.66 MPa, a Poisson's ratio of 0.45 and a density of 1062 kg/m^3 [18].

Boundary conditions

A real pulsatile flow velocity in the entrance of abdominal aorta of a healthy adult was measured via laser Doppler anemometry (LDA) and used in this study. Figure 6 shows the realistic waveform inlet velocity, *u(t)*, with a time period (t_p) of 0.82s .

The mean arterial pressure takes account of pulsatile blood flow in the arteries, and is the best measure of perfusion pressure to an organ [12]. For the main outlet boundary, a constant pressure of 11500 Pa is set which is the mean through aorta. A mean pressure of 11000 *Pa* is specified for the right and left renal arteries outlet pressure. An appropriate boundary condition is applied on walls to indicate the interfaces on which FSI occurs. This allows the transfer of fluid forces and solid displacements across the specified boundaries. The solid model corresponding to the vessel walls are assumed to be fixed at the outlet of renal arteries, because of their connection to the kidneys. The inlet and outlet of aorta are exposed to a boundary condition, such that only movement in the radial-tangential plane is allowed.

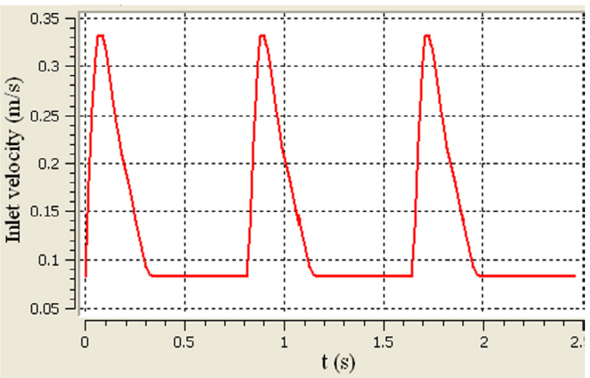

Figure 6: Time variation of the inlet velocity, *u(t)*

Results and discussion

Validation

To validate the methods employed in this study, a comparison with the numerical study by Chan *et al.* [19] is performed. Chan *et al.* [19]studied pulsatile blood flow in a flexible stenosed artery (Figure 7) and used a sinusoidal volumetric flow waveform of $4.3 \pm 2.6\, ml/s$ at the inlet with a period of $t_p = 0.345s$. A constant pressure of 4140 *Pa* was specified at the outlet.

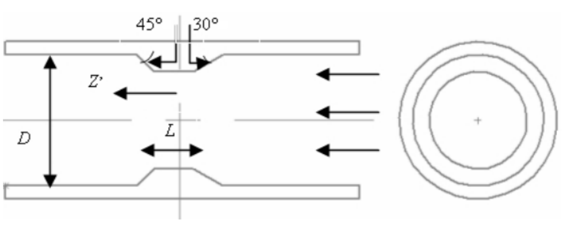

Figure 7: Stenosed artery uesd by Chan et al.[19] , *L = 1.5 mm*, *D = 5 mm* and *Z' = Z/D* is the normalized distance from the centre of stenosis.

The results for axial velocity profile at and wall shear stress for Carreau non-Newtonian model are presented in this section (Figures 8 and 9). The parameter t/t_p is used to describe a particular time in a cycle. The term t represents the time in seconds and t_p is the period of the flow cycle.

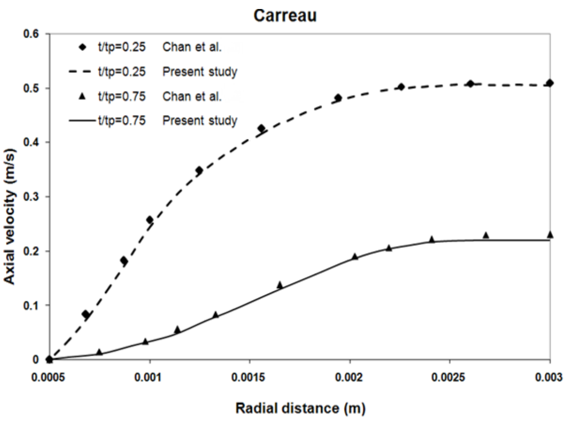

Figure 8: Axialvelocity profile at *Z' = 4.3*

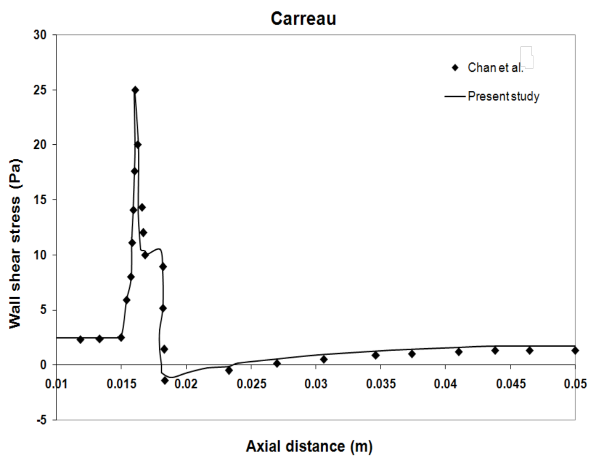

Figure 9: Wall shear stress along the axial distance at $t/t_p = 0.25$

According to these figures, acceptable agreement between the results is obtained.

Basic model results

Three different branch angles, i.e. 45°,90° and 135°, are considered for right renal arteryto investigate the angulation effects of stenosed renal arteries on blood flow characteristics. Simulations are carried out over at least three complete cycles to achieve a periodic solution and results are saved for the final cycle.

As pointed out earlier, the main goal of this study is to investigate the flow characteristics which are highly affected by renal branch angles as a critical parameter, particularly renal mass flow rate, that affects cardiac conditions and can finally result in hypertension. Therefore, we will mainly concentrate on blood velocity and mass flow rate and exclude other flow parameters such as shear stress, stream lines and vortex behavior from this study.

In this section, the results for velocity distributionsis depicted at selected times over cardiac cycle, *$t/t_p = 0.10$* and *$t/t_p = 1.00$*, corresponding to maximum and minimum inlet flow, respectively. In addition, right renal mass flow rate is plotted for three different branch angles over whole cardiac cycle.

Velocity

Plots of time-dependent velocity distribution at selected times for the three models, i.e. right renal angles of 45°, 90° and 135°, are shown in figures 10 to 12.

It is observed that high curvature of streamlines in the entrance of the right renal artery with the angle of 135° causes the flow velocity in this artery to be less than those of 45°and

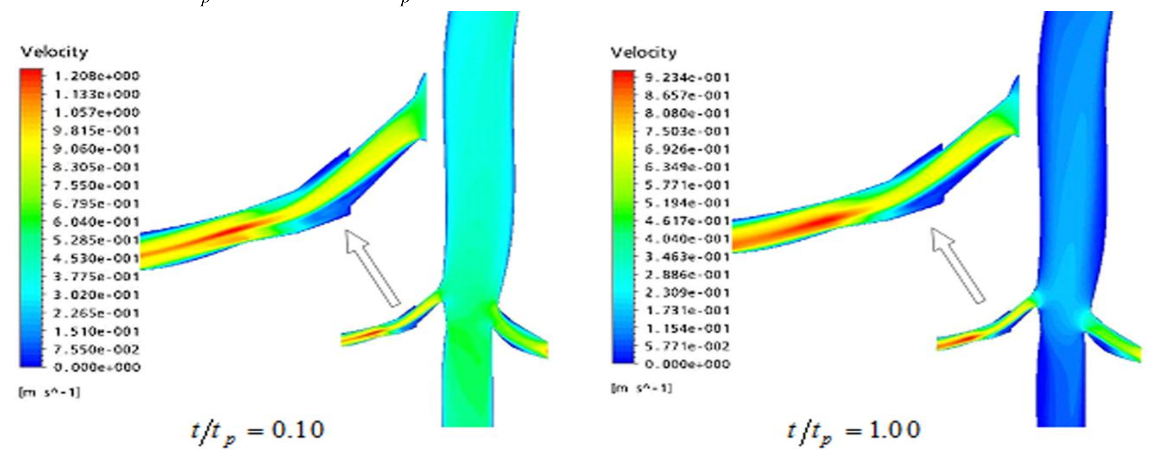

Figure 10: Velocity distribution at selected time frames in model with the right renal angle of 45°

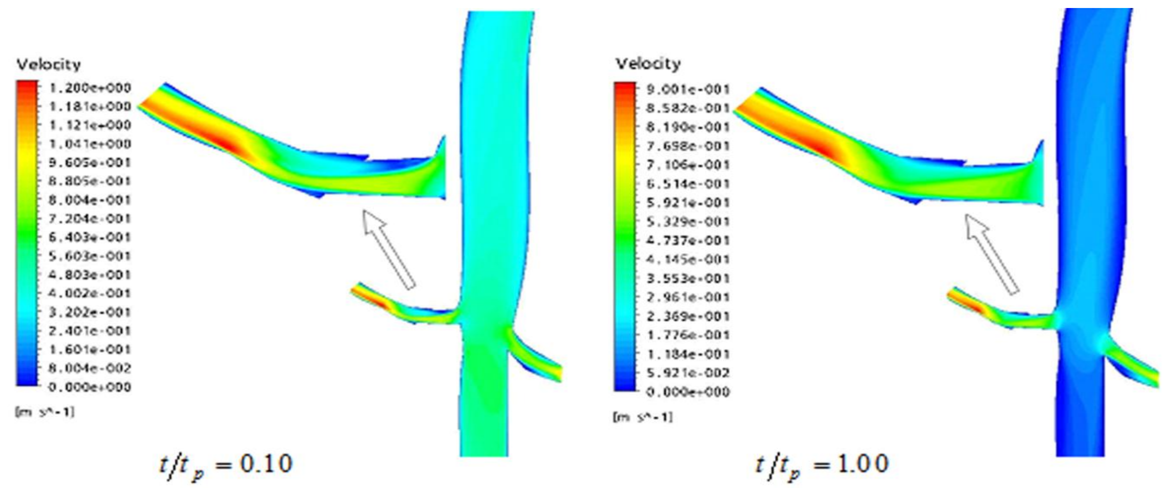

Figure 11: Velocity distribution at selected time frames in model with the right renal angle of 90°

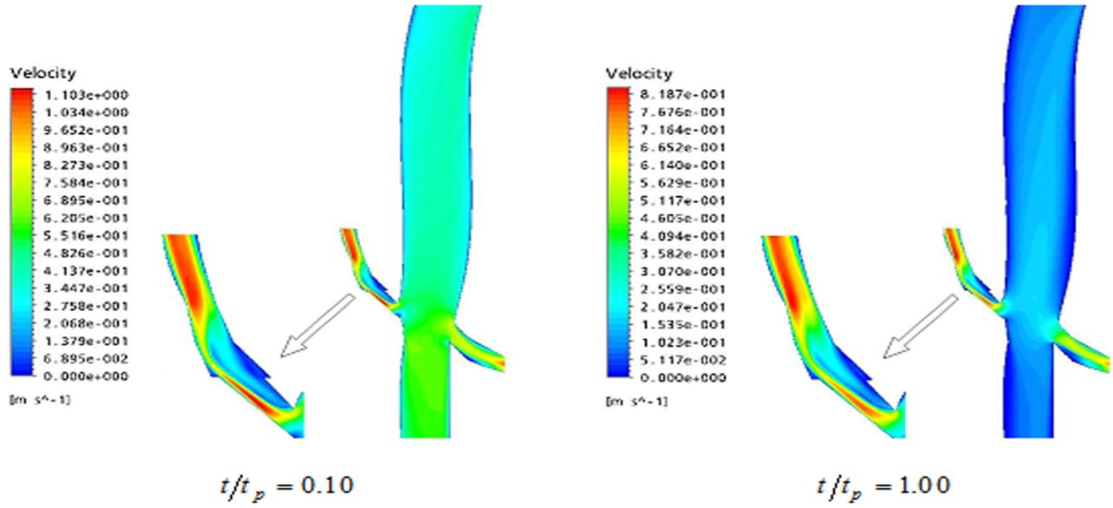

Figure 12: Velocity distribution at selected time frames in model with the right renal angle of 135°

90˚.

Mass flow rate

Figure 13 shows mass flow rate over one flow cycle through right renal artery with branch angles of 45˚, 90˚ and 135˚.It is obvious that streamlines in the entrance of right renal artery with the angle of 135˚ are highly curved in comparison with the two other branch angles and this causes the mass flow rate in this artery to be less than those of 45˚and 90˚. According to this figure, renal mass flow rate with the angle of 135˚ is approximately 22% less than 45˚. As mentioned before, response of the kidney to the decrease in renalmass flow is activation of the renin-angiotension system, which results in severe hypertension [9,11].

Conclusions

The purpose of this study was to investigate the angulation effects on blood flow velocity and renal mass flow rate in stenosed renal arteries. To achieve this, pulsatile non-Newtonian blood flow was simulated through a realistic model of abdominal aorta and renal arteries reconstructed from CT-scan images, considering an axisymmetric trapezium shape stenosis with area reduction of 45% in the entrance of right renal artery. The renal arteries had left and right branch angles of 53˚ and 45˚,

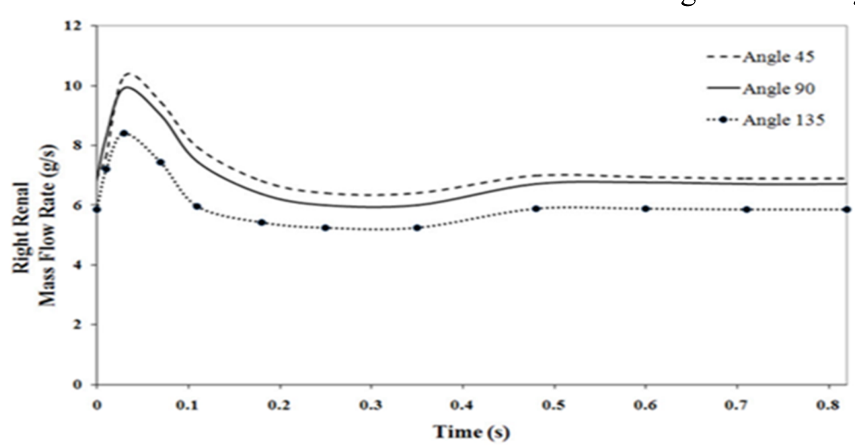

Figure 13: Mass flow rate over one flow cycle through right renal arterywith the angles of 45°, 90° and 135°

respectively in the realistic model. In addition, two other branch angles, i.e. 90° and 135°, were also considered for right renal artery to study the effects of angulation.

It was observed that high curvature of streamlines in the entrance of the right renal artery with the angle of 135° causes the flow velocity and mass flow to be less than those of 45°and 90°. For instance, mass flow rate in the renal artery with the angle of 135° is about 22% less than 45°.

It is concluded that renal branch angle is also a critical parameter which can affect blood flow characteristics through renal arteries. Large renal branch angle causes the arteries to be unable to deliver blood in the requisite amounts to the kidney, consequently, renal mass flow decreases. Kidney responds to counteract low blood flow by activating the renin-angiotension system which results in severe hypertension[9,11].

Conflict of Interest

None

References

1. Ku DN. Blood flow in arteries. *Annu Rev Fluid Mech.* 1997;**29**:399-434.
2. Arcangelo VP, Peterson AM. *Pharmacotherapeutics for Advanced Practice: A Practical Approach.* Philadelphia, Pa: Lippincott Williams & Wilkins; 2006. 959 p.
3. Carretero OA, Oparil S. Essential hypertension. Part I: definition and etiology. *Circulation.* 2000;**101**:329-35. PubMed PMID: 10645931.
4. Shetty R, Amin MS, Jovin IS. Atherosclerotic renal artery stenosis: current therapy and future developments. *Am Heart J.* 2009;**158**:154-62. doi: 10.1016/j.ahj.2009.05.025. PubMed PMID: 19619689.
5. Liang F, Yamaguchi R, Liu H. Fluid Dynamics in Normal and Stenosed Human Renal Arteries: an Experimental and Computational Study. *J Biomech Sci Eng.* 2006;**1**:171-82.
6. Kagadis GC, Skouras ED, Bourantas GC, *et al.* Computational representation and hemodynamic characterization of in vivo acquired severe stenotic renal artery geometries using turbulence modeling. *Med Eng Phys*. 2008;**30**:647-60. doi: 10.1016/j.medengphy.2007.07.005. PubMed PMID: 17714975.
7. Schoenberg SO, Bock M, Kallinowski F, Just A. Correlation of hemodynamic impact and morphologic degree of renal artery stenosis in a canine model. *J Am Soc Nephrol*. 2000;**11**:2190-8. PubMed PMID: 11095642.
8. Westenberg JJ, Wasser MN, van der Geest RJ, *et al.* Variations in blood flow waveforms in stenotic renal arteries by 2D phase-contrast cine MRI. *J Magn Reson Imaging*. 1998;**8**:590-7. PubMed PMID: 9626873.
9. Derkx FHM, Schalekamp MADH. Renal artery stenosis and hypertension. *The Lancet.* 1994;**344**:237-9.
10. Yamamoto T, Ogasawara Y, Kimura A, *et al.* Blood velocity profiles in the human renal artery by Doppler ultrasound and their relationship to atherosclerosis. *Arterioscler Throm Vasc Biol.* 1996;**16**:172-7. PubMed PMID: 8548419.
11. Mount P, Kumar SK, MacGinley R, Mantha M, Roberts M, Mangos G. Inhibition of the renin–angiotensin system. *Nephrology.* 2010;**15**:S234-S43. doi: 10.1111/j.1440-1797.2009.01246.x.
12. Ganong WF. *Review of medical physiology.* 14th ed. California: Appleton & Lange; 1989. 673 p.
13. Lai WM, Rubin D, Krempl E. *Introduction to Continuum Mechanics.* 3rd ed. Burlington: Elsevier Science; 1999. 552 p.
14. Ballyk PD, Steinman DA, Ethier CR. Simulation of non-Newtonian blood flow in an end-to-side anastomosis. *Biorheology.* 1994;**31**:565-86. PubMed PMID: 7833458.
15. Cho YI, Kensey KR. Effects of the non-Newtonian viscosity of blood in flows in a diseased arterial vessel. Part 1: Steady flows. *Biorheology.* 1991;**28**:241-62.
16. Johnston BM, Johnston PR, Corney S, Kilpatrick D. Non-Newtonian blood flow in human right coronary arteries: steady state simulations. *J Biomech.* 2004;**37**:709-20. doi: 10.1016/j.jbiomech.2003.09.016. PubMed PMID: 15047000.
17. Walburn FJ, Schneck DJ. A constitutive equation for whole human blood. *Biorheology.* 1976;**13**:201-10. PubMed PMID: 953256.
18. Giannakoulas G, Giannoglou G, Soulis J, *et al.* A computational model to predict aortic wall stresses in patients with systolic arterial hypertension. *Med Hypotheses.* 2005;**65**:1191-5. doi: 10.1016/j.mehy.2005.06.017. PubMed PMID: 16107302.
19. Chan W, Ding Y, Tu JY. Modeling of non-Newtonian blood flow through a stenosed artery incorporating fluid-structure interaction. *ANZIAM J.* 2007;**47**:507-23.